

Mitochondrial pathway-mediated apoptosis is associated with erlotinib-induced cytotoxicity in hepatic cells

XUEQIN CHEN, SHAOYU YANG, YUELONG PAN, XIN LI and SHENGLIN MA

Department of Medical Oncology, Hangzhou First People's Hospital,
Nanjing Medical University, Hangzhou, Zhejiang 310006, P.R. China

Received April 30, 2016; Accepted August 23, 2017

DOI: 10.3892/ol.2017.7359

Abstract. For advanced non-small-cell lung cancer (NSCLC) with mutations to the epidermal growth factor receptor (EGFR), EGFR tyrosine kinase inhibitors, including erlotinib are indicated for the first-line treatment. Liver injury is one of the multiple adverse effects of erlotinib and may affect its safety. The present study investigated the mechanism of erlotinib-induced hepatotoxicity *in vitro* and provided experimental evidence for the screening of potential hepatoprotectors. Erlotinib induced dose-dependent cytotoxicity in human L-02 hepatic cells 72 h after treatment. In other experiments, L-02 cells were treated with erlotinib for 48 h and thereafter exhibited typical features of apoptosis. Erlotinib caused alterations to nuclear morphology, including chromatin condensation and karyopyknosis; it also increased the fraction of late apoptotic cells and regulated apoptotic protein levels, activating caspase-3 and cleaving of poly-ADP-ribose polymerase. Furthermore, 48 h exposure to erlotinib disturbed mitochondrial function by decreasing the ratio of B-cell lymphoma 2 (Bcl-2) to Bcl-associated X proteins and reducing mitochondrial membrane potential. The results of this *in vitro* study indicate that erlotinib-induced hepatotoxicity may occur through mitochondrial-pathway-mediated apoptosis.

Introduction

Lung cancer is the leading cause of cancer mortality globally; 85-90% of cases of lung cancer were non-small-cell lung cancer (NSCLC) between 1975 and 2012 (1,2). During this time, ~80% of NSCLC cases were locally advanced (stage IIIA/B) or metastatic (stage IV), with poor prognosis (2). For advanced NSCLC, platinum-based doublet chemotherapy, the standard

treatment, has reached a plateau (3). The median survival time of NSCLC from 2001 to 2004 for stages IIIB/IV was <1 year and the 3- and 5-year survival rates were 4.3 and 2.8%, respectively (4). Precision medicine and individualized therapy are the emerging fields in cancer research, and multiple established and potential targets, including epidermal growth factor receptor (EGFR) and anaplastic lymphoma kinase genes, are the foundation of this therapy.

Multiple clinical trials indicate that, in comparison with chemotherapy, treatment with the tyrosine kinase inhibitor (TKI) erlotinib, which targets the EGFR, results in an improved response rate (RR) for advanced or metastatic NSCLC and can prolong progression-free survival (PFS), representing a valid treatment option (5,6). However, despite its benefits, erlotinib induces hepatotoxicity that can pose substantial harm to patients. The EORTC study (6) revealed that in Western countries, the incidence rates of all-grade and grade-3 liver enzyme elevation were 6 and 2%, respectively, among erlotinib-treated patients with advanced NSCLC with EGFR mutations. However, the incidence of hepatotoxicity is higher in Eastern countries. The OPTIMAL study (5) indicated that in Eastern countries, the incidence rates of all-grade, and grade-3/4 alanine transaminase (ALT) elevation were 37 and 4%, respectively, among erlotinib-treated patients with NSCLC with EGFR mutations. With such occurrence and occasionally serious severity, hepatotoxicity as a side effect of erlotinib is positively associated with the efficacy of erlotinib, and the survival of patients. Therefore, considering the requirement of long-term administration of EGFR-TKIs, including erlotinib, there is a requirement for studies on erlotinib-induced hepatotoxicity.

The mechanism of drug-induced liver injury (DILI) has not previously been completely elucidated. Mitochondrial injury has been proposed and acknowledged as one possible mechanism for DILI (7). Therefore, in the present study, the human hepatocyte L-02 cell line was used as an *in vitro* model to investigate whether the mitochondrial pathway of apoptosis was involved in erlotinib-induced hepatotoxicity.

Materials and methods

Drugs and chemicals. Erlotinib was obtained from Roche Diagnostics (Basel, Switzerland) and dissolved in DMSO (50 mmol/l stock solution). Erlotinib was stored at -40°C as

Correspondence to: Dr Shenglin Ma, Department of Medical Oncology, Hangzhou First People's Hospital, Nanjing Medical University, 261 Huansha Road, Hangzhou, Zhejiang 310006, P.R. China
E-mail: mashenglin@medmail.com.cn

Key words: erlotinib, hepatotoxicity, mitochondrial pathway, apoptosis, *in vitro* study, hepatocytes

frozen aliquots and the solution was thawed directly prior to the experiments. The chemical structure of erlotinib is presented in Fig. 1A.

Cell line and cell culture. L-02 cells, human hepatocytes, were purchased from Shanghai Institute of Biochemistry and Cell Biology (Shanghai, China). L-02 cells were maintained in complete RPMI-1640 media (Gibco; Thermo Fisher Scientific, Inc., Waltham, MA, USA) at 37°C under 5% CO₂ with 10% heat-inactivated fetal bovine serum (FBS; Invitrogen; Thermo Fisher Scientific, Inc.), containing 100 U/ml penicillin (Invitrogen; Thermo Fisher Scientific, Inc.) and 100 µg/ml streptomycin (Invitrogen; Thermo Fisher Scientific, Inc.).

Cell proliferation assay. The sulforhodamine B (SRB) colorimetric assay (Sigma-Aldrich; Merck KGaA, Darmstadt, Germany) was used to evaluate cell proliferation. L-02 cells (3x10³ cells/well) were cultured in 96-well plates and exposed to erlotinib (0, 1.56, 3.13, 6.25, 12.50, 25.00 or 50.00 µM) for 72 h. The cells were then fixed with 10% trichloroacetic acid (Sigma-Aldrich; Merck KGaA) for 1 h at 4°C. Once the cells had been stained with SRB for 30 min at room temperature and bound SRB had been dissolved with 10 mmol/l Tris-base, a multi-well spectrophotometer was used to measure the absorbance at 510 nm. Calculation of the cell survival rate was according to the following formula: A510 treated cells/A510 control cells x100.

DAPI staining assay. L-02 cells (3x10⁴ cells/well) cultured exponentially in 6-well plates were exposed to erlotinib (0, 6.25, 12.50 or 25.00 µM) for 48 h. To study cell morphology, the cells were rinsed in PBS followed by fixation with 0.1% Triton X-100 for 15 min. Next, DAPI (2.0 µg/ml; Sigma-Aldrich; Merck KGaA) was used to stain the cells for 15 min. All steps were performed at room temperature. The morphology of cell nuclei was examined by fluorescence microscopy (magnification, x100).

Apoptosis detection by flow cytometry. An Annexin V-fluorescein isothiocyanate (FITC) /propidium iodide (PI) apoptosis detection kit (Invitrogen; Thermo Fisher Scientific, Inc.) was used to measure apoptosis rate. L-02 cells (3x10⁴ cells/well) were harvested 48 h after treatment with erlotinib (0, 6.25, 12.50, 25.00 µM). L-02 cells were washed twice with cold PBS, 1x10⁶ cells/ml were resuspended in 1X binding buffer of the kit and 100 µl cell suspension was transferred to a 5-ml culture tube. In the dark, the transferred suspension was stained with 5 µl Annexin V-FITC and 5 µl PI at 25°C for 15 min. Cell apoptosis was detected using a FACSCalibur flow cytometer (BD Biosciences, Franklin Lakes, NJ, USA) with BD FACSDiva Software (version 8.0.1) within 1 h.

Mitochondrial membrane potential ($\Delta\Psi_m$) evaluation by JC-1 stain. L-02 cells were inoculated into 6-well plates (1.5x10⁴ cells/well) for 24 h at 37°C. Following treatment with erlotinib (0, 6.25, 12.50, 25.00 µM) for 48 h, L-02 cell suspension was prepared in PBS (500 µl) and stained with 2.5 µl JC-1 (20 µg/ml) for 30 min at 37°C under 5% CO₂. As a cationic dye, once in the mitochondria, JC-1 shifts its fluorescence emission from green to red, from 525±10 to 610±10 nm, as it

accumulates owing to the high membrane potential. The cell suspension was sampled as 1x10⁴ cells/sample. A FACSCalibur flow cytometer was used to analyze the fluorescence emission. The fluorescence intensity ratio of red/green decreases when mitochondrial depolarization occurs.

Western blot analysis. Briefly, protein was extracted from L-02 cells in lysis buffer (50 mmol/l Tris-HCl, 150.0 mmol/l NaCl, 1 mmol/l EDTA, 1 mmol/l phenylmethylsulfonyl fluoride, 1% NP-40, 0.1% SDS, 0.5% deoxycholic acid, 2.0 µg/ml aprotinin, 0.02% NaN₃). Lysates were centrifuged (1x10⁴ x g) at 4°C for 15 min. Protein expression (20 µg/lane) was detected by SDS-PAGE (8-15% gel), and proteins were electroblotted onto polyvinylidene fluoride membranes (EMD Millipore, Billerica, MA, USA). Primary and horseradish peroxidase (HRP)-conjugated secondary antibodies (Southern Biotech, Birmingham, AL, USA) were used to probe proteins. The primary antibodies used were: B-cell lymphoma 2 (Bcl-2; cat. no. 2872) and cleaved caspase-3 (cat. no. 9961) purchased from Cell Signaling Technology, Inc. (Danvers, MA, USA); cleaved poly (ADP-ribose) polymerase (PARP; cat. no. sc-56196), Bcl-associated X (Bax; cat. no. sc-4239) and β-actin (cat. no. sc-1615) purchased from Santa Cruz Biotechnology, Inc. (Dallas, TX, USA). HRP-labeled secondary antibodies (GAR007, GAM007, RAG007) were purchased from MultiSciences Biotech Co., Ltd. (Hangzhou, China). The primary and secondary antibodies were diluted into 1:1,000 and 1:5,000, respectively. Incubation occurred for 2 or 0.5 h at room temperature and washing for 5 min/wash for three washes. An enhanced chemiluminescence detection system (Biological Industries, Beit Haemek, Israel) was used for protein detection.

Statistical analysis. SPSS version 18.0 (SPSS, Inc., Chicago, IL, USA) was used for statistical analyses. Survival rates were presented as mean ± standard deviation and analyzed using two-way analysis of variance. P<0.05 (two-way) was considered to indicate a statistically significant difference.

Results

Erlotinib induces cytotoxicity in L-02 cells. Cell viability was assessed using a SRB colorimetric assay following treatment of L-02 cells with erlotinib (0, 1.56, 3.13, 6.25, 12.50, 25.00, 50.00 µM) for 72 h. As presented in Fig. 1B and C, a dose-dependent inhibition of L-02 cell proliferation was detected in L-02 cells following exposure to erlotinib for 72 h (P<0.05). The percentage of cells that survived (compared with untreated control cells) was 70.31±4.90 and 48.64±6.83% at the lowest (P=0.03), and highest (P=0.003) concentration tested, respectively. The growth of L-02 cells following the 72-h treatment was analyzed using light microscopy. Cellular swelling, a cloudy cytoplasm, slow cell growth and impaired cell adherence were observed (Fig. 1D).

Erlotinib induces apoptosis in L-02 cells. Following treatment of L-02 cells with 6.25, 12.50 and 25.00 µM erlotinib for 48 h, DAPI staining was used to detect variations in the nucleus morphology caused by apoptosis. Upon examination by fluorescence microscopy, L-02 cells treated with 12.50 µM erlotinib exhibited chromatin condensation and karyopyknosis,

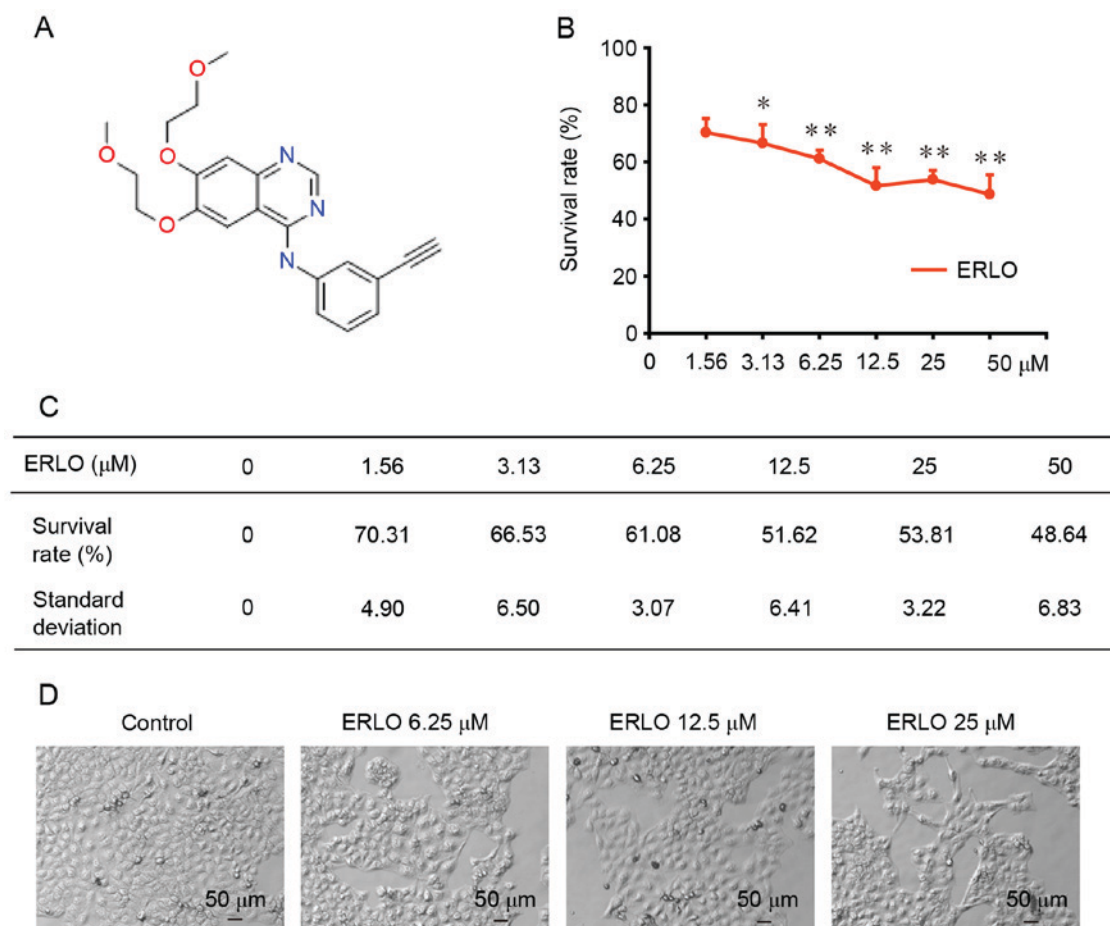


Figure 1. Erlotinib inhibits the proliferation of L-02 cells in a dose-dependent manner. (A) The chemical structure of erlotinib. (B) L-02 cells were treated with erlotinib (0, 1.56, 3.13, 6.25, 12.50, 25.00, 50.00 μ M) for 72 h and a sulforhodamine B assay analyzed cell survival. * $P<0.05$, ** $P<0.01$ vs. control (0 μ M). (C) Survival rate figures presented in (B). (D) Growth of L-02 cells under a light microscope. ERLO, erlotinib.

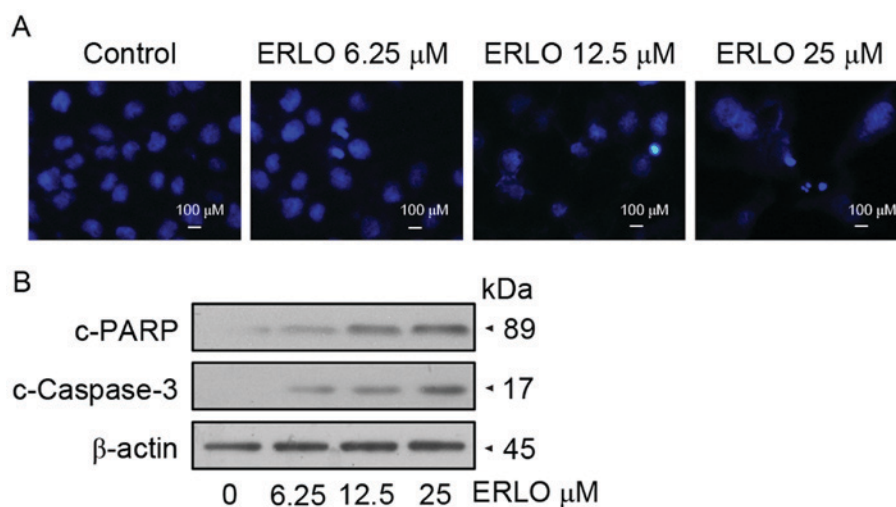


Figure 2. Erlotinib causes chromatin condensation, karyopyknosis and upregulated apoptosis proteins dose-dependently in L-02 cells when L-02 cells were exposed to increasing doses of erlotinib for 48 h. (A) Fluorescence microscopic images of the nuclear morphology of L-02 cells, stained with DAPI. (B) The upregulation of c-caspase-3 and c-PARP analyzed by western blotting. Data are representative of three independent experiments. ERLO, erlotinib; c-, cleaved; PARP, poly (ADP-ribose) polymerase.

which are typical apoptotic phenomena. Further marked nuclear pyknosis was observed at a concentration of 25.00 μ M, indicating the dose-dependent effect of erlotinib on the apoptosis of L-02 cells (Fig. 2A). Furthermore, detection of

apoptotic protein expression was performed by western blot analysis. In concordance with the morphological changes, the levels of cleaved caspase-3 and cleaved PARP increased in a dose-dependent manner in treated cells, indicating the

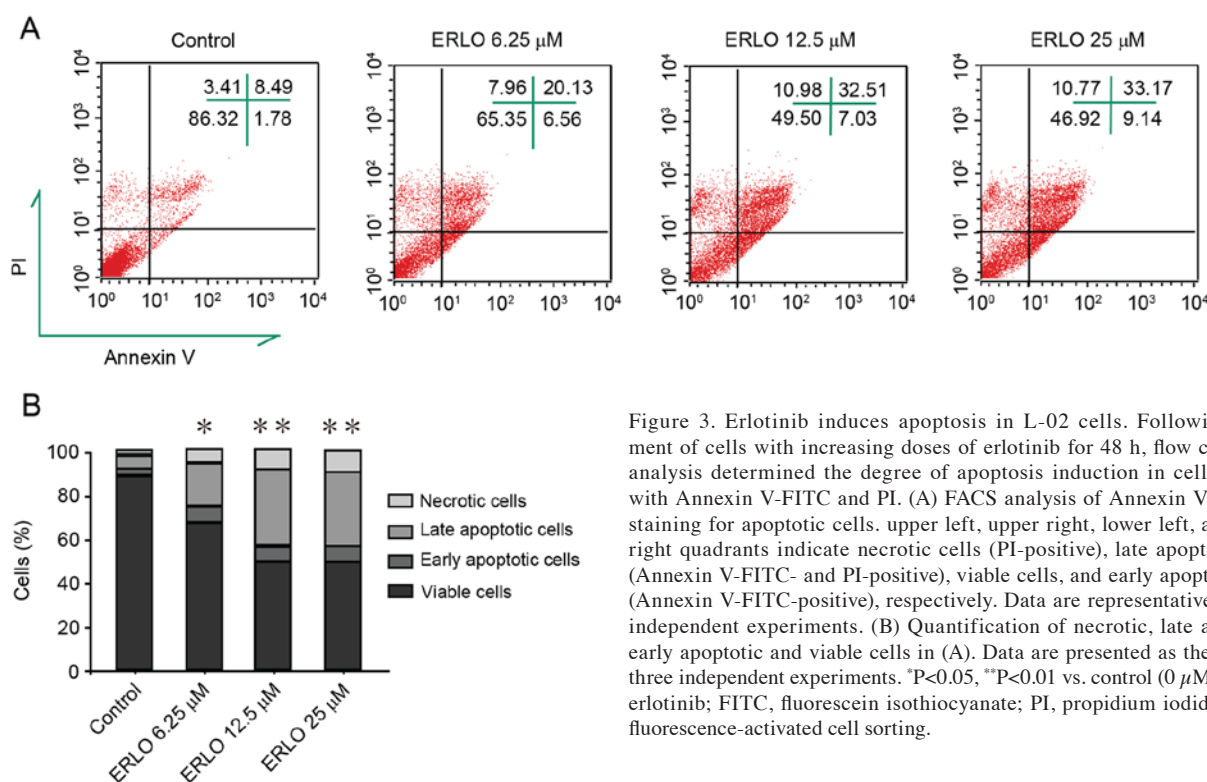


Figure 3. Erlotinib induces apoptosis in L-O2 cells. Following treatment of cells with increasing doses of erlotinib for 48 h, flow cytometry analysis determined the degree of apoptosis induction in cells stained with Annexin V-FITC and PI. (A) FACS analysis of Annexin V-FITC/PI staining for apoptotic cells. upper left, upper right, lower left, and lower right quadrants indicate necrotic cells (PI-positive), late apoptotic cells (Annexin V-FITC- and PI-positive), viable cells, and early apoptotic cells (Annexin V-FITC-positive), respectively. Data are representative of three independent experiments. (B) Quantification of necrotic, late apoptotic, early apoptotic and viable cells in (A). Data are presented as the mean of three independent experiments. * $P < 0.05$, ** $P < 0.01$ vs. control (0 μ M). ERLO, erlotinib; FITC, fluorescein isothiocyanate; PI, propidium iodide; FACS, fluorescence-activated cell sorting.

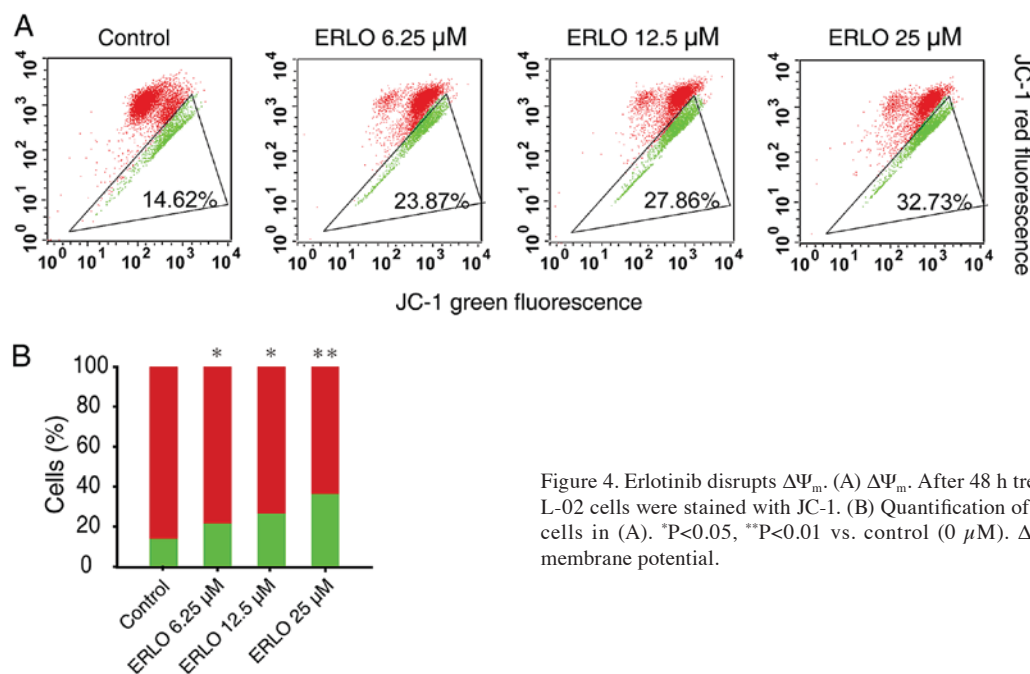


Figure 4. Erlotinib disrupts $\Delta\Psi_m$. (A) $\Delta\Psi_m$. After 48 h treatment of erlotinib, L-O2 cells were stained with JC-1. (B) Quantification of high- and low- $\Delta\Psi_m$ cells in (A). * $P < 0.05$, ** $P < 0.01$ vs. control (0 μ M). $\Delta\Psi_m$, mitochondrial membrane potential.

upregulation of apoptotic proteins (Fig. 2B). Subsequently, measurement by flow cytometry of the apoptotic rate of cells stained with Annexin V-FITC/PI was performed. Compared with the control, the late apoptotic rate in erlotinib-treated cells increased significantly and dose-dependently ($P < 0.05$; Fig. 3). These results revealed that apoptosis contributes to erlotinib-induced hepatotoxicity.

Mitochondrial pathway is involved in erlotinib-induced apoptosis. During drug-induced apoptosis, mitochondrial changes

are the key events. Therefore, the function of mitochondria in erlotinib-induced apoptosis was investigated. JC-1 staining and western blot analysis was used to examine the variation of $\Delta\Psi_m$, and associated protein expression in L-O2 cells treated with erlotinib (0, 6.25, 12.50 and 25.00 μ M) for 48 h. Using JC-1 staining, treated cells exhibited a decreased red/green fluorescence intensity ratio in line with the increasing concentration of erlotinib ($P < 0.05$), which indicated that erlotinib treatment induced a dose-dependent loss of $\Delta\Psi_m$ and mitochondrial depolarization (Fig. 4). Since the mitochondrial

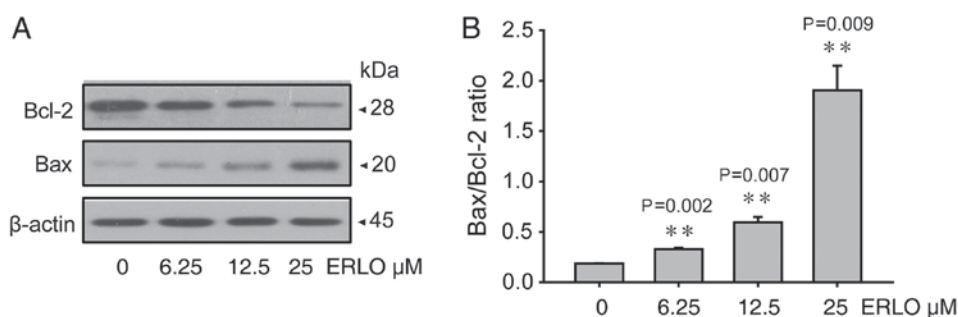


Figure 5. Altered levels of Bax and Bcl-2 in L-O2 cells. (A) Protein expression of Bcl-2 and Bax in L-O2 cells analyzed by western blot analysis after cells were inoculated with erlotinib for 48 h. (B) Quantification of Bcl-2 and Bax expression in (A). ** $P < 0.01$ vs. control (0 μM). Bcl-2, B-cell lymphoma 2; Bax, Bcl-associated X; ERLO, erlotinib.

pathway of apoptosis is regulated by proteins of the Bcl-2 family (8), the levels of the pro-apoptotic Bax and anti-apoptotic Bcl-2 proteins were analyzed. The levels of Bcl-2 protein decreased whereas those of Bax increased in L-O2 cells 24 h after erlotinib treatment (6.25, 12.50, 25.00 $\mu\text{mol/l}$), in a dose-dependent manner (Fig. 5). The present study indicated that the mitochondrial pathway may be involved in apoptosis induced by erlotinib.

Discussion

The mechanism of drug-induced liver injury (DILI) has not been completely elucidated. Russmann *et al* (9) suggested that the mechanism may include specific injury 'upstream' and unspecific 'downstream' events. The upstream events of DILI are initial hepatocyte injury caused by sophisticated interactions between hereditary and environmental risk factors, whereas the downstream events involve the equilibrium between the processes of injury and protection in mitochondrion. To study the mechanism of DILI, a three-step working model was proposed (9). First, drugs associated with DILI and their reactive metabolites directly cause cellular stress, inhibit mitochondrial functions and activate specific immune responses. Secondly, mitochondrial permeability transition (MPT) caused by initial injury may proceed through an intrinsic pathway by activating cascades of intracellular stressors and an extrinsic pathway modulated by cytokines, and immune reactions. Finally, depending on ATP availability, MPT may result in necrosis or apoptosis.

Liver injury is a frequent side effect in patients undergoing long-term erlotinib treatment. Hepatotoxicity can influence the efficacy of erlotinib and survival (10). Thus, the purpose of the present study was to investigate the potential mechanism of erlotinib-induced hepatotoxicity via *in vitro* experiments with L-O2 cells. The present study revealed that, in L-O2 cells, cell viability decreased dose-dependently and cell morphology was altered 72 h after erlotinib treatment. As a form of programmed cell death, apoptosis is associated with DILI. In the present study, DAPI staining revealed chromatin condensation and karyopyknosis in the nucleus, and increased apoptosis in a dose-dependent manner in L-O2 cells following erlotinib treatment. Similar results have been reported in hepatocytes upon treatment with other drugs, including 17-demethoxy-reblastatin, schisandrin B and saikosaponin D and (11-13). PARP is a DNA repair enzyme whose

cleaved form contributes to apoptosis owing to drug toxicity. Caspase-3 is responsible for PARP cleavage during the early stage of apoptosis (14). Therefore, increased levels of cleaved caspase-3 and cleaved PARP lead to apoptosis. In the present study, cleaved caspase-3 and cleaved PARP protein expression levels increased following erlotinib treatment. These data demonstrated that erlotinib-induced hepatotoxicity occurs through the process of apoptosis.

Generally, the biological mechanism of apoptosis is composed of an extrinsic pathway that is death-receptor-dependent and an intrinsic pathway that is mitochondrial-dependent (15,16). The two pathways are involved in drug-induced apoptosis (13,17). A collapse of the $\Delta\Psi_m$ was observed alongside an alteration of Bax and Bcl-2 protein expression during the apoptosis of hepatocytes induced by saikosaponin D (13). Data from the present study demonstrated that erlotinib-treated hepatocytes exhibit significantly decreased $\Delta\Psi_m$ and Bcl-2 protein levels, but increased Bax expression, all in a dose-dependent manner. These results indicated that erlotinib-induced apoptosis may proceed through the mitochondrial-dependent pathway.

Acetaminophen (APAP) is one of the most common causes of DILI owing to its wide use as an analgesic (18). The mechanisms of APAP-induced hepatotoxicity include the damage of reactive drug intermediates/binding/adducts, mitochondrial dysfunction, nuclear DNA damage, karyorrhexis and inflammation (19). Additionally, hepatoprotective factors, including heat shock protein exhibit a protective function in hepatotoxicity (20). Certain studies (21,22) have provided evidence that mitochondrial dysfunction and damage is involved in APAP hepatotoxicity in humans, and inflammation is necessary for recovery and regeneration, whereas apoptosis has only a minor function. By contrast, the present study demonstrated that erlotinib-induced hepatotoxicity involved mitochondrial damage accompanied with apoptotic phenomena, including chromatin condensation, nuclear fragmentation, and caspase expression and cleavage.

Nowadays, TKIs are increasingly applied in clinical practice and TKI-induced hepatotoxicity is common (23). However, studies of TKI-induced hepatotoxicity are relatively rare and the mechanisms involved are poorly understood. Xue *et al* (24) reported that mitochondria-mediated cell death pathway serves an essential function via oxidative stress, and activation of nuclear factor erythroid 2-related factor 2 and the mitogen-activated protein kinase pathway in dasatinib-induced hepatotoxicity. Researchers from the

same group also identified that autophagy protects against dasatinib-induced hepatotoxicity by activating p38 signaling in liver tissues and primary cultured rat hepatocytes (25). The current study demonstrated that erlotinib induces apoptosis in hepatocytes with a correspondent decrease in the $\Delta\Psi_m$ and alterations to protein expression typical of the mitochondrial apoptotic pathway. These results indicated that the potential mechanism of erlotinib-induced hepatotoxicity may involve the mitochondrial apoptosis pathway.

The evidence provided by the present study expands the understanding of the fundamental mechanism of TKI-induced hepatotoxicity. Further *in vivo* research is; however, required to support these observations.

Acknowledgements

The present study was supported by the Zhejiang Provincial Foundation of National Science (grant nos. LZ13H160001 and LY14H160006) and the Health Foundation of Hangzhou City Zhejiang Province (grant no. 2015Z003).

References

1. Siegel RL, Miller KD and Jemal A: Cancer statistics, 2016. *CA Cancer J Clin* 66: 7-30, 2016.
2. Howlader N, Noone AM, Krapcho M, Garshell J, Miller D, Altekruse SF, Kosary CL, Yu M, Ruhl J, Tatalovich Z, *et al* (eds): SEER cancer statistics review 1975-2012. Natl Cancer Inst, Nov 18, 2015.
3. Iranzo V, Bremnes RM, Almendros P, Gavilá J, Blasco A, Sirera R and Camps C: Induction chemotherapy followed by concurrent chemoradiation for patients with non-operable stage III non-small-cell lung cancer. *Lung Cancer* 63: 63-67, 2009.
4. Ozkaya S, Findik S, Dirican A and Atici AG: Long-term survival rates of patients with stage IIIB and IV non-small cell lung cancer treated with cisplatin plus vinorelbine or gemcitabine. *Exp Ther Med* 4: 1035-1038, 2012.
5. Zhou C, Wu YL, Chen G, Feng J, Liu XQ, Wang C, Zhang S, Wang J, Zhou S, Ren S, *et al*: Erlotinib versus chemotherapy as first-line treatment for patients with advanced EGFR mutation-positive non-small-cell lung cancer (OPTIMAL, CTONG-0802): A multicentre, open-label, randomized, phase 3 study. *Lancet oncol* 12: 735-742, 2011.
6. Rosell R, Carcereny E, Gervais R, Vergnenegre A, Massuti B, Felip E, Palmero R, Garcia-Gomez R, Pallares C, Sanchez JM, *et al*: Erlotinib versus standard chemotherapy as first-line treatment for European patients with advanced EGFR mutation-positive non-small-cell lung cancer (EORTAC): A multicentre, open-label, randomized phase 3 trial. *Lancet Oncol* 13: 239-246, 2012.
7. Russmann S, Kullak-Ublick GA and Grattagliano I: Current concepts of mechanisms in drug-induced hepatotoxicity. *Curr Med Chem* 16: 3041-3053, 2009.
8. Leanza L, Henry B, Sassi N, Zoratti M, Chandy KG, Gulbins E and Szabó I: Inhibitors of mitochondrial Kv1.3 channels induce Bax/Bak-independent death of cancer cells. *EMBO Mol Med* 4: 577-593, 2012.
9. Russmann S, Jetter A and Kullak-Ublick GA: Pharmacogenetics of drug-induced liver injury. *Hepatology* 52: 748-761, 2010.
10. Teo YL, Ho HK and Chan A: Risk of tyrosine kinase inhibitors-induced hepatotoxicity in cancer patients: A meta-analysis. *Cancer Treat Rev* 39: 199-206, 2013.
11. Zhao S, Li H, Jiang C, Ma T, Wu C, Huo Q and Liu H: 17-Demethoxy-reblastatin, an Hsp90 inhibitor, induces mitochondria-mediated apoptosis through downregulation of Mcl-1 in human hepatocellular carcinoma cells. *J Bioenerg Biomembr* 47: 373-381, 2015.
12. Zhang Y, Zhou ZW, Jin H, Hu C, He ZX, Yu ZL, Ko KM, Yang T, Zhang X, Pan SY and Zhou SF: Schisandrin B inhibits cell growth and induces cellular apoptosis and autophagy in mouse hepatocytes and macrophages: Implications for its hepatotoxicity. *Drug Des Devel Ther* 9: 2001-2027, 2015.
13. Chen L, Zhang F, Kong D, Zhu X, Chen W, Wang A and Zheng S: Saikosaponin D disrupts platelet-derived growth factor- β receptor/p38 pathway leading to mitochondrial apoptosis in human LO2 hepatocyte cells: A potential mechanism of hepatotoxicity. *Chem Biol Interact* 206: 76-82, 2013.
14. Oliver FJ, de la Rubia G, Rolli V, Ruiz-Ruiz MC, de Murcia G, Murcia JM: Importance of poly(ADP-ribose) polymerase and its cleavage in apoptosis. Lesson from an uncleavable mutant. *J Biol Chem* 273: 33533-33539, 1998.
15. Kaiser WJ, Upton JW, Long AB, Livingston-Rosanoff D, Daley-Bauer LP, Hakem R, Caspary T and Mocarski ES: RIP3 mediates the embryonic lethality of caspase-8-deficient mice. *Nature* 471: 368-372, 2011.
16. Guha M, Maity P, Choubey V, Mitra K, Reiter RJ and Bandyopadhyay U: Melatonin inhibits free radical-mediated mitochondrial-dependent hepatocyte apoptosis and liver damage induced during malarial infection. *J Pineal Res* 43: 372-381, 2007.
17. Zhang F, Chen L, Jin H, Shao J, Wu L, Lu Y and Zheng S: Activation of Fas death receptor pathway and Bid in hepatocytes is involved in saikosaponin D induction of hepatotoxicity. *Environ Toxicol Pharmacol* 41: 8-13, 2016.
18. Lee WM: Etiologies of acute liver failure. *Semin Liver Dis* 28: 142-152, 2008.
19. McGill MR and Jaeschke H: Mechanistic biomarkers in acetaminophen-induced hepatotoxicity and acute liver failure: From preclinical models to patients. *Expert Opin Drug Metab Toxicol* 10: 1005-1017, 2014.
20. Williams CD, McGill MR, Farhood A and Jaeschke H: Fas receptor-deficient lpr mice are protected against acetaminophen hepatotoxicity due to higher glutathione synthesis and enhanced detoxification of oxidant stress. *Food Chem Toxicol* 58: 228-235, 2013.
21. McGill MR, Sharpe MR, Williams CD, Taha M, Curry SC and Jaeschke H: The mechanism underlying acetaminophen-induced hepatotoxicity in humans and mice involves mitochondrial damage and nuclear DNA fragmentation. *J Clin Invest* 122: 1574-1583, 2012.
22. Hu J, Ramshesh VK, McGill MR, Jaeschke H and Lemasters JJ: Low dose acetaminophen induces reversible mitochondrial dysfunction associated with transient c-Jun N-terminal kinase activation in mouse liver. *Toxicol Sci* 150: 204-15, 2016.
23. Chen X, Yang S and Ma S: Drug induced hepatotoxicity in targeted therapy for lung cancer. *Zhongguo Fei Ai Za Zhi* 17: 685-688, 2014 (In Chinese).
24. Xue T, Luo P, Zhu H, Zhao Y, Wu H, Gai R, Wu Y, Yang B, Yang X and He Q: Oxidative stress is involved in Dasatinib-induced apoptosis in rat primary hepatocytes. *Toxicol Appl Pharmacol* 261: 280-291, 2012.
25. Yang X, Wang J, Dai J, Shao J, Ma J, Chen C, Ma S, He Q, Luo P and Yang B: Autophagy protects against dasatinib-induced hepatotoxicity via p38 signaling. *Oncotarget* 6: 6203-6217, 2015.



This work is licensed under a Creative Commons Attribution-NonCommercial-NoDerivatives 4.0 International (CC BY-NC-ND 4.0) License.